IRANIAN JOURNAL OF PHYSICS RESEARCH

Iranian Journal of Physics Research, Vol. 14, No. 3, 2014

Multichannel Kondo approach to the cuprate and recent laser ARPES data

M A Mojumder

JNI RCMPS, Chittagong University, Chittagong, Bangladesh

(Received 4 May 2013 , in final from 5 January 2014)

Abstract

The existing theoretical approaches have been unable to confront the large corpus of outstanding data on the cuprate superconductor in a persuasive and unified manner. There is a general opinion now growing that these theories miss some essential points. We propose one based on multichannel Kondo effect that is physically justifiable and confronts the data adequately. In addition to earlier data, the definitive proof of involvement of this effect has been now provided by the numerical agreement of the characteristic Kondo temperatures with the fluctuation frequencies at which Eliashberg function peaks. It is, therefore, suggested that the theory of multichannel Kondo effect be accepted as the correct theory of underdoped cuprate.

Keywords: cuprates physics, high-T_c superconductivity, multichannel Kondo effect, pseudogap, of two channel Kondo effect

1. Introduction

The focus of the study of the doped cuprate (HTC), having shifted to the study of their physical properties, has helped to uncover many unexpected metallic properties that defy straightforward theoretical understanding. Investigation of these highly correlated metals has led to the notion that a fundamentally new state of matter different from the conventional Landau Fermi liquid exists in the phase diagram.

A new name, non-Fermi liquid, has been coined for it. Precise data on ρ_{ab}, crystal resistivity in the plane, [1- 4], NMR [5,6], the pseudogap (PG) [7-9] ,the dome [8]and the pairing interaction [10, 12] have helped us to establish the multichannel Kondo effect [13-15] as quenching and delocalising the magnetic Mott insulator parent crystal. From a very recent Laser ARPES data [16-19], the fluctuation energies at which the unexplained peaks of the Eliashberg function appear have been shown by us to correspond to the mutichannel Kondo temperatures, section 3.4. This provides the latest and most direct support to Kondo effect. We discuss the central issues of the effect in brief, justify it theoretically, and point out how the Kondo fixed points (KFP) enable the simplest and the most straightforward rationalisation of the outstanding unexplained data. It allows one to predict data as well. We mainly analyse the data on common representative HTC's for the sake of simplicity .

Though the conventional (single channel)Kondo model was considered for its possible applicability to the study of the HTC and discarded, the multichannel Kondo model has never been seriously considered. In fact,this model was thought of as an academic curiosity only and is not well-known. The evidence presented in this work showed that this model is stable enough to be effective. And our exhaustive search of the literature has not produced a single piece of data that can not be understood in a simple manner by using this model. The mathematical aspects of the multichannel theory at T=0 has been well-established since 1995; we have extended it to T>0 by using the Matsubara formalism. They have been presented in brief in section 3.1. Most of the major topics of the area referred to briefly have already been discussed in detail individually in separate publications cited here.

In this work, we ignore the distinction of Kondo transition (T=0) and Kondo crossover at higher temperature. Because of the very large energy scale T_K of the HTC, section 3.1, the difference between the two is insignificant at the usual working temperatures of about 100 K.

2. Current theories

The currently popular theories of the HTC have failed to explain the vast volume of data in a unified and convincing manner. The much-discussed 2D Hubbard

Current address: Flat No.201,'Vars Tranquil', 1st A Main, ST Bed Layout, Kormangala 4th Block, Bangalore -560034, India.

model and the related t-J model, taken with the resonance valence bond (RVB) model could explain the early data. But it has been inadequate in respect of the more recent and complex data which have been rarely addressed by any theory in a unified and consistent manner. Though some researchers in the area have expressed dissatisfaction none have proposed a satisfactory alternative approach. The more recent developments of the orbital selective Mott transition for multiband crystals and fractionalized Fermi liquid have, despite their elaborate and complex nature, not improved the situation. Validity of the numerous claims made in respect of the RVB spin liquid model has been challenged [20] in detail. The marginal Fermi liquid (MFL)theory and its recent form, the circulating current (CC) theories [21], were partially successful vis-a-vis some data but, broadly speaking, inadequate and inconclusive. Their main deficiency has been the complete neglect of the high energy scales for which there is enough evidence. An example of their severe shortcoming vis-à-vis recent INS data once believed to strongly support these theories appears in section 3.4. In contrast, nobody has found a single piece of data that can not be explained in a straightforward manner in Kondo approach.

2. 1. The doped cuprate and the two channel Kondo model

The local moment description for the Cu^{+2} spin 1/2 has been argued [22] to be correct, and the conclusion is generally accepted. $U > \Delta_{CT}$ being a general finding for the HTC, Kondo effect is suggested. U and Δ_{CT} are respectively, Hubbard correlation and charge transfer gap. It has been noted [23] that $W_{cu\mathbf{3}d} < W_{O\mathbf{2}p}$, as known to be true for the HTC, favours the Kondo channel over Mott for the changes of the parent crystal under doping; W is the bandwidth. That the parent crystal undergoing 'Mott' transition is actually a doping-induced disordered paramagnetic insulator[24,25] rather than an antiferromagnetic (AFM) insulator is now known. On the basis of numerical [26] and other [27] evidence from experimental data, we assume the transition from the parent crystal leads to one channel Kondo fixed point (1CKFP), a Fermi liquid, at lower temperatures. The transition occurs to 2CKFP at higher temperature for say, $T > \tilde{T}_{KC}$. $\tilde{T}_{KC}$ is the channel transition temperature defined in section 3.1. There is a proof of the existence of a Fermi liquid at low temperature and doping via quantum oscillations in the pseudogap(PG), section 4.2 [27].

The 2CKFP Emery-Kivelson (EK) Green function [28], section 3.1., manifests a variety of non-Fermi liquid properties, [13, 14, 29] e.g.

(a) $\frac{C_V}{T} \propto \ln T$

(b) $\chi_{zz} \propto \ln(\frac{\tilde{T}_K}{T}), \quad \eta_\perp{}^2 << \frac{T}{\tilde{T}_K};$

(c) $S = (\frac{1}{2})k_B \ln 2, \quad \eta_\perp << \frac{T}{\tilde{T}_K};$

(d) ρ_{ab} & $\rho_c \propto \left|\ln(\frac{T}{\tilde{T}_K})\right|, \quad T \to 0 \quad ,$ (1)

where S is the entropy. There are others among these two important early data that were compelling, definitive and unique signatures of 2CKFP in the 'normal' state: the resistivity rule, $\rho_{ab} \propto \left|\ln(T/\tilde{T}_K)\right|, \quad T \to 0$, eq. (1 (d)), [1, 3] and $S = (1/2)k_B \ln 2, T \to 0$. The nature of the variation [6] of the NMR parameter, $\mathrm{R} \equiv 1/T^{63}T_1$ with temperature remained a mystery for a long time till we applied the notion of Kondo channel transition ,Section 3.1, to understand it. T_1 is the transverse NMR relaxation time and $\tilde{T}_K$ the crystal coherence temperature of the d-wave pairing band. Verification [24] of the residual entropy for the HTC is not direct ;it only shows the full entropy to be $k_B \ln 2$ / Cu ion. By assuming two channel Kondo effect, one obtains the residual entropy $(1/2)k_B \ln 2$, a signature of the two channel effect, a result that sustains the assumption. Oxygen atoms harbouring the doped holes Kondo interact with Cu along the ...Cu-O-Cu...antinodal direction. In the nodal ...Cu-Cu-Cu... direction, on the other hand, Kondo effect is almost nil.

The existence of multiple transition lines [30,31], figure.1, persuaded us early to think of the multichannel Kondo effect. The Cu3d crystal field (CF) multiplet has been suggested on the basis of band structure studies [32] to be separated into two groups, planar and axial. We believe they respectively undergo two channel Kondo effect (one channel Kondo effect) at T_K (some lower temperature) that results in d-wave (s-wave) pairing band. These two incoherent bands become coherent respectively, at $\tilde{T}_K$ and at a much lower temperature T_0. The two bands (gaps) coexist in the normal state at the lower temperatures (dome); this is sometimes disbelieved despite numerous evidence [33-35]. Two energy scales have been detected in the dome which can be identified as $\tilde{T}_K$ and T_0, respectively. STM data as well as the finding of a high scaling temperature for the Hall data [36] indicate a high scaling temperature which we identify with Kondo temperature.

2. 2. The two bands and two liquids

Fermi liquid and non-Fermi liquid respectively, support the s-wave- and d-wave superconductivities, the latter incoherent and along the antinode at higher temperature, and the former coherent and along the node at lower temperature. The d-wave pairing band arises [32] from the ground level planar hybrid orbital comprising the $Cu3d_{x^2-y^2}$ and $Cu3d_{xy}$ orbitals. Correspondingly, the s-wave pairing band arises from the axial hybrid

comprised of the excited level orbital $Cu3d_{3z^2-r^2}$, the apical oxygen orbital $O_a{}^2p_z{}^-$, $Cu4s$ orbital, and the metallic orbital from the insulating layer. This band becomes stronger at lower temperatures particularly, at the high doping levels of the dome. The s-wave pairing band and the corresponding superconductivity, being subdominant in the basal plane, are generally shut out by the dominant d-wave pairing band and the corresponding superconductivity at higher temperatures.

The delocalised planar $Cu3d_{x^2-y^2}$ orbital being positively charged, naturally forms the positively charged d-wave pairing band Fermi surface. But the delocalised axial orbital $Cu3d_{3z^2-r^2}$, though positively charged, joins the negatively charged s-wave pairing band Fermi surface. This happens as all the other orbitals that together constitute the axial s-wave pairing band appear to have a greater weight of negative charge particularly due to the Cu4s orbital. The presence of a distinct s-wave pairing band and the corresponding superconductivity commencing at T_c are specifically supported by data, as mentioned. Physically, the two channel Kondo effect requires two degenerate CF levels which can be quenched by electrons(holes) simultaneously. Here, the levels $Cu3d_{x^2-y^2}$ and $Cu3d_{3z^2-r^2}$ are effectively degenerate in the context of the much larger width of the O2*p* band.

3. Two channel Kondo effect

Via the perturbative renormalisation group (PRG) theory [15] an 'impurity' with spin ½ as in Cu^{+2} undergoing two channel Kondo effect has been argued to end up as a quenched and delocalised impurity with the same spin ½, and half the spectral weight left unquenched at $T\to 0$. PRG theory gives a ground state with a finite degeneracy at $T\to 0$ with entropy $S = (1/2)k_B \ln 2$. The two channel effect overscreens the 'impurity' moment while the effective exchange flows to an intermediate coupling fixed point. We use the following standard Hamiltonian [13,14] for the single 'impurity' two channel Kondo model,

$$H_2 = \sum_a \sum_{\sigma=1,2} [H_0(\psi_{a\sigma}\dagger, \psi_{a\sigma}) + , \sum_{i=x,y,z} J_a{}^i S^i \psi_{a\alpha}\dagger(0)\sigma_{\alpha\beta}{}^i \psi_{a\beta}(0)], \quad (2)$$

$$\psi_{a\alpha}{}^\dagger(0)\sigma_{\alpha\beta}{}^i\psi_{a\beta}(0) \equiv \sigma^i, \ a = 1,2.$$

Here a=(1,2) for doubly-degenerate conduction band with kinetic energy $H_0(\psi^\dagger, \psi) = \sum_k \varepsilon_k \psi_k{}^\dagger \psi_k$. a=(1,2) is also the channel index of the impurity. The first term in the square bracket is the kinetic energy; the second is the Kondo term. S =½ is the pseudospin of the Cu^{2+} ion, the 'impurity'. σ is the spin of the conduction electrons and is 'up' or 'down'. This is the Emery-Kivelson (EK) model [28] which is unstable by definition.

This equation was solved [13,14] by generalization of the known method for solving the one channel case. The authors found the model, eq. (2), equivalent to a generalised resonant level model; comparison of order by order expansion of the two models showed their identity. This identity occurs only when the Kondo coupling J^z is restricted to the value $J^z = 2\pi v_F$; v_F is the Fermi velocity of the conduction band. Simplification was achieved by restricting to the Kondo scattering phase shift π/2 for a single channel case. Thus the generalised resonant level equation in a solvable form equivalent to eq. (2) was found.

In this case the system ,by construction unstable, would choose asymptotically the stronger Kondo coupling to achieve the full normal screening of the 'impurity'. This would be the Kondo channel transition, a true second order transition, at $\tilde{T}_{KC}$ or decay of the 2CKFP to the stable 1CKFP. An assumed but plausible mechanism to represent this decay has been to add an extra piece of channel anisotropic Hamiltonian as a perturbation to bare eq. (2). The resulting channel symmetry-breaking Hamiltonian [13,14] is quantified in terms of a finite coordinate-specific multiplicative parameter λ, $0 < \lambda_i < 1$, $i = x, y, z$. For two channels and $\lambda_\perp \neq 0$, one has $\delta = \pi/4$. This model has been diagonalised giving the Kondo impurity Green function $G(t) = -i\langle T_\tau[D(t)^\dagger D(t)]\rangle$, $D^\dagger = (d^\dagger, d)$,

$$G(\omega) = (\frac{1}{2})\left(\frac{\tau_0 - \tau_1}{\omega + iT_K \operatorname{sgn}\omega} + \frac{\tau_0 + \tau_1}{\omega + i\lambda_\perp{}^2 T_K \operatorname{sgn}\omega}\right), \quad (3)$$

for frequency much smaller than the conduction bandwidth. τ_i are the Pauli matrices.

Eq. (3) is the sum of two Lorentzians of widths T_K and $\lambda_\perp{}^2 T_K$ .The second term decouples from doped holes in the limit $\lambda_\perp \to 0$ and tends to a δ-function of frequency. On performing analytic continuation, $\omega \to i\omega_n$ in the Matsubara formalism the first term of eq. (3) becomes

$$G(i\omega_n) = \frac{(\frac{1}{2})(\tau_0 - \tau_1)}{i\omega_n + i\tilde{T}_K \operatorname{sgn}\omega_n}, \ 0 < T << \tilde{T}_K,$$

$$\omega_n = (2n+1)\pi T, n = 0, \pm 1, \pm 2, \pm 3 \quad . \quad (4)$$

This is the EK model, $T \neq 0$, [28], for $\lambda_\perp = 0$ and $\delta = \pi/2$ for an individual channel. The doped holes, keeping coupled to the EK function, make it move away from 2CKFP to 1CKFP. The rate of this decay is very large for $\lambda_\perp = 0$ but is finite for finite $\lambda_\perp$. For $\omega \to 0$ the δ-function term of eq. (3) takes away half the spectral weight which is unquenched, a characteristic of 2CKFP. In real HTC crystal, the decay of 2CKFP via a channel transition is very slow [15] ('arrest') as $T_K < \Delta E$ which makes 2CKFP

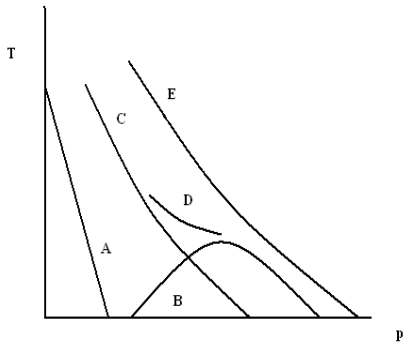

Figure 1. p-T phase diagram of the doped crystal.

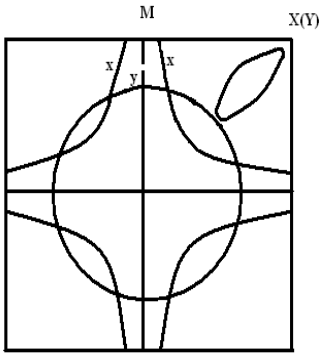

Figure 2. Quantum oscillation in $YBCO_{6.45}$:123.

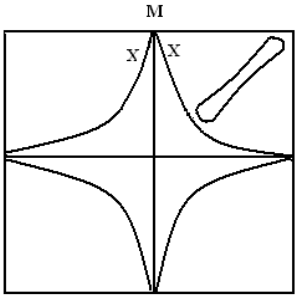

Figure 3. Quantum oscillation in YBCO: 124.

stable enough to dominate the physics. ΔE is the relevant splitting of CF levels and they are known.

3. 1. The quantum critical point

Quantum criticality arises from competing ground states and exists at the T=0 point of a phase transition line between these ground states. It implies that the system at this T=0 quantum critical point (QCP) behaves the same on average regardless of the time and length scales at which it is observed. It is believed to develop very large correlation length and very long correlation time that cause the transition at this point. If the transition is continuous as in Kondo transition, it is driven, instead of thermal fluctuations, by nondissipative quantum fluctuations of both spin and charge character at the QCP in both space and time. This nature of the transition is inherent in the togetherness of spin and charge flucuations. That the two, the Anderson and the Kondo equations, can be mapped to each other is known. That most often spin fluctuation is detected rather than the charge fluctuation (plasmon) due to the easier detection of spin fluctuation.

Experimentally, the linear rule $\rho_{ab} \propto T$, a characteristic of the 'strange metal' of Anderson has two mysteries inherent to it. One is about the rule being valid usually up to more than 1000K which equals $\tilde{T}_K$ for optimal doping. This signifies the presence of at least one high energy scale and shows the notion of scale-invariance proposed in the MFL theory is wrong. The other is the presence of a point of inflexion in the $\rho_{ab}(T)$ curve whose origin, even now, is not understood by anybody,to my knowledge.Our derivation [37] of the linear rule for 2CKFP shows explicitly that the constant of proportionality in the linear rule has a factor $\tilde{T}_K$ which accounts for the very long linearity. Also, the channel transition switching, section 3.1, between $\tilde{T}_K$ and $\tilde{T}_{KC}$ causes the inflexion. That the conventional notion of quantum critical behaviour being scale invariant is not valid for the HTC is further confirmed by the absence of a single master curve for all values of ω/T, ref. [38]. It is obvious that, contrary to common belief, the linear rule $\rho_{ab} \propto T$ does not follow from the basic one parameter temperature-scaling hypothesis of quantum criticality.

The assumption of multichannel Kondo effect is consistent with the definition of the Kondo QCPs [39] as the T=0 Kondo phase transition that occurs between the overscreened 2CKFP and the paramagnetic phase (1CKFP) under change of doping at T=0. For the usual p-T phase diagram, figure 1. the point p=0.19 at T=0 satisfies this criterion. This QCP seems strange as it exists inside the dome without being directly involved in the superconductivity. In our Kondo approach, however, the matter is simple in the sense that the QCPs has no direct relationship with superconductivity, whether s-wave- or d-wave. One recalls that the pseudogap has weights of both the 2CKFP and 1CKFP, section 4.2, and the regime of the dome has both 2CKFP, p>0.19, and 1CKFP, p<0.19. Outside the pseudogap and the dome the presence of the 2CKFP d-wave superconductivity [40] and 1CKFP s-wave superconductivity are of pristine origin.

3. 2. ARPES and other data vis-a-vis Kondo effect

ARPES data directly showing [41] Kondo effect is the appearance of four Fermi resonances of maximum local density of states (LDOS) in place of the Fermi surface at low temperature in the pseudogap (PG) regime. Kondo approach identifies the four LDOS peaks with those expected to arise from the four Kondo resonances along the nodal directions for the 'descendent' s-wave pairing band, section 4.2. But due to the curvature of the d-wave pairing band Fermi surface, at 2CKFP near the point

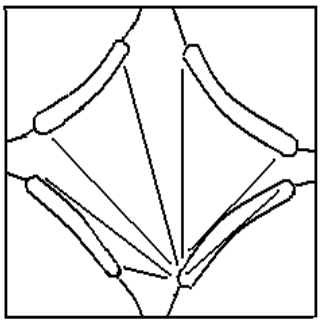

Figure 4. Origin of 'Octet'.

$\bar{M}$ along the antinodal direction it shall have eight resonances, figures 2 and 3. This is so because of the bifurcation of each Kondo resonance into two. The octet Phenomenology [42,43], figure 4, around the consequences of scattering between the eight resonances can be explained on the above basis. This is one of the most direct experimental evidence for the 2CKFP. The empirical development in this area would have been easier with the present understanding.

ARPES data-fitting analysis [44] done at different temperatures finds a very large imaginary part Σ_2 of the self-energy of the carrier,

$$\Sigma_2(\hat{q},\omega;T) \propto -\tilde{\Gamma}(\hat{q}_F) + \Sigma_2{}'(\omega;T) \quad . \tag{5}$$

Σ_2 is strongly anisotropic in the basal plane. Here $\left|-\tilde{\Gamma}(\hat{q}_F)\right| >> \left|\Sigma_2{}'(\omega;T)\right|$; the left term exists almost only in the antinodal direction. Ignoring the right term which is small in a good crystal, one identifies $\tilde{\Gamma}(\hat{q}_F) = \tilde{T}_K(\hat{q}_F)$. $\tilde{T}_K(\hat{q}_F)$ is the self-energy due to Kondo effect. One concludes that planar anisotropy is due to the planar variation of self-energy from two channel effect. This is basically of Kondo origin.

3. 3. Eliashberg function and Kondo temperatures

Writing eq. (4) in the real frequency domain, we calculate the polarization(fluctuation) $\Pi(\omega,T)$ of fermions from which one obtains,

$$\mathrm{Im}\,\Pi(\omega,T) = -N_0\pi(\frac{\omega}{\tilde{T}_K})(\frac{T}{\tilde{T}_K})^2,$$

$$\mathrm{Re}\,\Pi(\omega,T) = (\frac{N_0\pi}{2})(\frac{\omega}{T_K})^2(\frac{T}{\tilde{T}_K})^2, \tag{6}$$

Up to second orders in $\omega/\tilde{T}_K$ and $T/\tilde{T}_K$. Eq.(6) is the fundamental hypothesis of MFL theory with T replaced by $\tilde{T}_K$. Eq. (6) with $EF_n \propto -|g|^2\,\mathrm{Im}\,\Pi(\omega)$ by definition, ref. [19], leads to eq. (7) below. (Sign reversal is due to convention).

$EF_n \equiv (\alpha^2\tilde{F}(\omega))_n$ is the Eliashberg function in the normal phase. α and ω are respectively the coupling and the fluctuation frequency. $\tilde{F}(\omega)$ is the fluctuation propagator of the mediating boson. $(\alpha^2\tilde{F}(\omega))_n$ differs from $(\alpha^2\tilde{F}(\omega))_S$ by $\sim\Delta/\tilde{T}_K << 1$ which is ignored. $\Pi(\omega)$ being momentum-independent, g is a constant. So,

$$EF_n \propto \mathrm{Im}\,\Pi(\omega) \propto (\frac{\omega}{T_K}), \quad T < T_K,$$

$$EF_n \propto (\frac{\omega}{\tilde{T}_K}), \quad T < \tilde{T}_K, \tag{7}$$

$$EF_n \propto (\frac{\omega}{\tilde{T}_{KC}}), \quad T < \tilde{T}_{KC}.$$

EF_n peaks at frequencies given by $T_K, \tilde{T}_K$ and $\tilde{T}_{KC}$; they appear when respectively,

$\omega \to T_K$, $\tilde{T}_K$ and $\tilde{T}_{KC}$. The peaks rise linearly with ω followed by a sharp drop to a uniform background. These peaks indicate pairing of fermions via mediation of bosons of energies at which the peaks appear. In refs. [16-19] EF_n has been evaluated by the authors from their Laser ARPES data in this manner. Direct detection of $\tilde{T}_{KC}$, $\tilde{T}_K$ and T_K via computation has been claimed because their values so obtained agree with the above data. This signals the fundamental role of the pairing bosons (plasmons)which correspond [45] to $T_K, \tilde{T}_K$ and $\tilde{T}_{KC}$. The detection of $T_K, \tilde{T}_K$ and $\tilde{T}_{KC}$ amounts to the detection of two channel Kondo effect and is the most direct proof of its presence.

The CC-θ_{II} theory, the generalised form of the MFL theory, predicts for the PG phase three weakly dispersive collective modes [21,46] for Hg1201 crystal, of which only the lowest, $\tilde{T}_{KC} \approx 55$ meV agrees with INS data for YBCO123. YBCO123 and Hg1201 have almost the same characteristic temperatures. Even if there were full agreement discrimination via INS data [47] between Kondo spin-like and orbital-like magnetic structure is impossible in CC-θ_{II} theory. The other two modes detected in INS corresponding to T_K and $\tilde{T}_{KC}$ escape the CC-θ_{II} theory. INS data for mildly underdoped Bi2212 [48-50] show three peaks ≈ 15 meV, 50 meV and 400 meV which accord with those detected by optical spectroscopy [51]. Incoherence induces jitter for the 400 meV which regardless has a sharp cut-off. If the large width of this peak induces any doubt about its validity one may derive the assurance of validity of our claim by comparing the INS data with those from ref. [51].

4. d-Wave-and s-wave superconductivities

The characteristic d-wave pairing [40] follows simply from two channel Kondo effect using the typical band dispersion. The small momentum transfer in the collisions used in the derivation follows from the fact that all the carriers have [52] effectively $\vec{q} \approx 0$ via umklapp. That a bosonic excitation (plasmon) with energy $\tilde{T}_K$ and $\tilde{T}_{KC}$ exists in the normal state in the

antinodal direction has been known from the preceeding section. $\tilde{T}_K$ and $\tilde{T}_{KC}$ have respectively values ~ 1500K and 100K,a result that is in agreement with later data [53, 54]. The characteristic properties of d-wave superconductivity [40] and the experimental detection of the plasmons are important supports of the two channel Kondo model.

Insufficient electrical screening of the oxygen atoms makes it possible for the acoustic phonon to couple with the oxygen ion to form the ionic plasmon [55]. There is evidence for the existence of the heavier ionic plasmon which has characteristics different from the usual electronic plasmon. This ionic plasmon is expected to correspond to T_0 because it is likely to be the energy scale of s-wave pairing, $T_0 > E_F$. Kondo effect at 1CKFP involves Coulomb interaction; the higher order Coulomb interaction considered to be the residual effect and represented by the ionic plasmon would be expected to provide the basic pairing in s-wave band Fermi liquid. Our estimated boson excitation is expected to be such an ionic plasmon, $\omega_p \approx T_0 \approx 200\,\mathrm{K}$, e.g, in the LSCO crystal. To our best knowledge, this plasmon has not yet been detected.

There are experimental evidences for the ionic plasmon. There is no conventional isotope effect in the HTC; the detected isotope effect has been attributed to only oxygen isotope. The experimentally known mass enhancement of s-wave pairing band Fermi liquid is about 9% [56, 57]. Kondo bonding between the electron and the oxygen atom induces this nonadiabaticity. This large nonadiabaticity is a departure from the Migdal-Eliashberg paradigm not usually expected in solely phonon-driven superconductivity [58]. This indicates the need to look for a suitable alternative.

Under the mediation of the ionic plasmon arising from the oxygen lattice in the underdoped regime up to about Tc, the pairing vertex of the axial s-wave band Fermi liquid reads under RPA [55],

$$\Gamma_i(\vec{q},\omega) = \frac{\dfrac{e^2}{4\pi q^2}}{1-(\dfrac{e^2}{4\pi q^2})\,\mathrm{Re}\,\Pi_i(\vec{q},\omega)}\quad , \tag{8}$$

This pairing vertex reads in the lowest approximation using the expression for $\Pi_i(\vec{q},\omega)$, the ionic plasmon propagator [55],

$$\Gamma_i(\vec{q},\omega_p) \approx \frac{-1}{\mathrm{Re}\,\Pi_i} \approx -(\frac{m_i}{n_i})(\frac{\omega_p}{q})^2, \qquad q = q_{BZ} \approx 10^7 \text{ units.} \tag{9}$$

As a numerical estimate using the calculated value of ω_p at the zone boundary, one has $\mathrm{Re}\,\Pi_i \approx 10^{34}$ units. We use only the ionic plasmon propagator as the most dominant at low temperature. There is a net Coulomb repulsion at the lowest order between the s-wave quasiparticles and so there is no crystal instability despite the attraction leading to pairing. The vertex has strong dependence on momentum and frequency, and so leads to a retarded attractive pairing in momentum space which gives BCS-like s-wave superconductivity. Ionic plasmon frequency is $\omega_p \propto (n_i/m_i)^{1/2}$ and $T_C \propto \omega_p$ from elementary theory [55] But at higher doping, for $T_C > \tilde{T}_{KC}$ Tc tracks the energy scale of T_0. This gives the typical shape of the dome.

For $T > \tilde{T}_{KC}$, the pure two channel Kondo regime, one has a coexistence of d-wave and s-wave bands which respectively, support the d-wave and s-wave superconductivities. The Brillouin zone-averaged T_d is close to but less than $\tilde{T}_K$ [40] while s-wave condensation occurs at $T_c^{\max} \approx 90$ K. This is again not a universality but only an approximation; its exact value depends on the out-of-plane structure as explained in an important case in the next para. In the pseudogap regime where the pristine d-wave band and its 'descendent' s-wave band, section 4.2, coexist the respective d-wave and s-wave pairing condensations occur at other temperatures.

Pairing via spin fluctuation pairing has been ruled out [19] for HTC. The $T_C^{\max}$ mentioned above is in accord with data for the common HTC but not for all. Though the extra contribution by a suitable c-axis optical phonon has been suggested this approach appears unable to deal with the important cases. It is highly likely that the extra input is provided by a c-axis ionic plasmon in crystals with varying distances of the apical O from the plane. One example of the effect is the very sharp rise of Tc^{max} for the single-layer $HgBa_2CuO_4$ to about 90K from about 40K for La_2CuO_4. The distance from Cu(2) to apical O for the above two cuprates are respectively, 2.8Å and 2.4 Å. It is known that for Kondo effect in such cases there is an optimal separation where the effect attains a sharp maximum. Just as Kondo effect in the HTC introduces a large Kondo temperature and a corresponding plasmon one expects, by analogy, an apical plasmon to exist due to Kondo effect between Cu(2) and O. This apical ionic plasmon would provide the extra contribution to the planar pairing ionic plasmon to produce the much higher T_c. To our best knowledge, the relevant study has not yet been carried out.

4. 1. Pseudogap and superconductivity

The problem of the PG, figure 5, has been considered the most crucial problem of the HTC and the key to the understanding of the HTC. The PG supports the pristine d-wave pairing band at 2CKFP and the Kondo-quenched s-wave pairing band at 1CKFP. It has been defined as a gap in the DOS or a general reduction of the DOS at the Fermi level of the carriers in the underdoped regime at $T < \tilde{T}_{KC}(p)$; $\tilde{T}_{KC}(p)$ is the onset of the channel transition from 2CKFP to 1CKFP. It harbours a wide

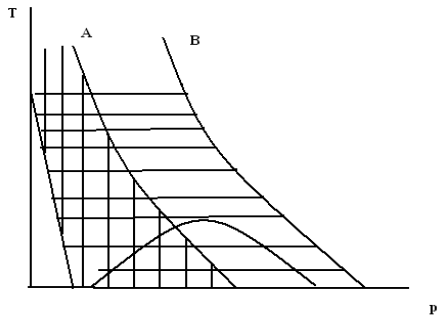

Figure 5. The cross-hatched pseudogap regime.

range of anomalies [59, 60] in the magnetic, charge transport, thermodynamic, and optical properties of the normal state. $\tilde{T}_{KC}$ meets the p-axis at p=0.19 and intersects the dome at about 90K. PG regime supports the coexistence of d-wave superconductivity at 2CKFP in the normal state persisting below $\tilde{T}_{KC}$ and its 'descendent', the s-wave superconductivity (1CKFP) condensing at say, $T_{dyn} \leq \tilde{T}_{KC}$. There are experimental supports for both these facts. The full gapping of the latter, now taken synonymous with the PG, has also been detected by ARPES [61] near E_F at low temperature. STM [62] shows random mixture of two kinds of nanocrystalline droplets of d-wave superconductivity and the PG (the s-wave superconductivity).

Inclusion of the second order perturbation correction [28] enables one to show $1/T_1 \propto -1/\tilde{T}_K$ which proves that as $\tilde{T}_K \to \tilde{T}_{KC}$, T_1 drops precipitately. T_1 is the transverse NMR relaxation time. This result has been detected many times. The central point is that in the PG the d-wave pairing band and its 'descendent' s-wave pairing band are distinct from the s-wave pairing band in the dome. This last s-wave pairing band is responsible for T_c. The PG and the dome are in distinct superconducting phases. These results directly confirm our proposal that the multichannel Kondo effect is the fundamental mechanism for the cuprate.

4. 2. Quantum oscillations

de Haas-van Alfven (dHvA)- and Shubnikov-de Haas (SdH) oscillation experiments performed on the same crystals, YBCO: 124 [63] and $YBCO_{6.45}$ [64] as well as studies of Hall resistivity [65] and Hall constant R_H(T) [66] have generally produced consistent data indicating well-defined, coherent and closed Fermi surfaces being responsible for them. These surfaces are actually Fermi pockets accounting for only about 2% of the sizes of the Fermi surfaces. Our conclusion has been that the pockets arise from Kondo resonances of the closed electronic Fermi surfaces of the s-wave pairing band and further surfaces created by scattering of the Kondo resonances. Though the electronic pocket is the general rule for the HTC the hole pocket is an exception for YBCO:124. It arises from the one channel Kondo transition from YBCO:124 parent crystal.

Quantum oscillation data have been interpreted successfully via the Liftshitz –Kosevich theory which shows them occuring in clean 2D Fermi liquids. The size of electronic Fermi pockets in the PG is an apparent violation of the Luttinger sum rule. Kondo effect and the scattering loss from Kondo resonances clarifies this problem. The detection of quantum oscillations in the PG is a clear vindication of our prediction that a Fermi liquid exists in the PG. The one channel Kondo transition from the parent crystal and the channel transition from higher temperature are consistent situations.

4. 3. The Fermi arc

It is the arc of the Fermi contour of this band straddling the nodal point symmetrically that disappears at very low temperature [67] but covers the whole of the contour at $T = T_d$. This is detected in the dome and the PG and is formed in the d-wave superconducting regime. This change in the arc length happens due to the change in the gap length; wherever the gap disappears the arc of the Fermi surface makes an appearance. It arises from the condensation temperature T_d of the d-wave pairing band being determined by the gap size which is variable for d-wave superconductivity. The Fermi arc becomes detectable usually in the $T < \tilde{T}_{KC}$ PG regime due to reduced Kondo scattering .

5. Magnetoresistance and thermal Hall conductivity

We have calculated a few magnetic properties as examples of the versatility and effectiveness of our approach. Calculatation of planar magnetoresistene(MR) has been done [68] using the standard expression for MR and writing it in terms of the Green function, eq. (4). This gives

$$MR \equiv \frac{\Delta\rho_{xx}}{\rho_0} = \left(\frac{15}{16}\right)$$

$$(\frac{\omega_C}{\tilde{T}_K})^2(\frac{1}{\tilde{T}_K})^2(\frac{1}{2m})^2(\frac{\pi}{a})^4[1-(\frac{148}{45})\pi^2 r^2] \qquad (10)$$

$$\equiv MR(T=0)u,\ u \equiv 1/(1+aT^2+a^2T^4),\ a \equiv (\frac{148}{45})\frac{\pi^2}{\tilde{T}_K{}^2},$$

up to $\vartheta(T/\tilde{T}_K)^4$. In eq. (10) at the channel transition $\tilde{T}_K \to \tilde{T}_{KC}$ MR would rise sharply. We have compared with eq. (10) the significant available data for both optimally-doped and overdoped YBCO:123, and an optimally doped LSCO crystal [69] and have found excellent agreement.

Calculation [70] of thermal Hall conductivity yields,

$$\kappa_{xy} = T(\frac{8\pi}{3})(\frac{1}{\tilde{T}_K{}^2})(\frac{\omega_c}{\tilde{T}_K})(\frac{1}{2m})^2(\frac{\pi}{a})^4(1-14\pi^2 r^2),$$

$$\omega_c \equiv \frac{eH}{mc} \quad . \qquad (11)$$

We found excellent agreement with data in this case as well.

Using the procedure parallel to the above calculations

we have computed other transport coefficients, e.g., Hall constant [71] and Nernst constant [52]. There is a hitherto mysterious piece of Hall data that at low temperature and higher doping close to about p=0.3 the sign of Hall constant switches from positive to negative . The $Cu4s$ orbital of high spectral weight, expected to be an important constituent [32] of the axial hybrid beyond optimal doping, is responsible for it even before the phase point crosses from inside to outside the dome at $p\approx$ 0.3, figure 1. Regarding the Nernst constant our calculations show its value to rise to its maximum at about 140 K followed by a trailing off to zero as the temperature is raised to $\tilde{T}_K$. It is surprising that the proposition of vortex formation at $T > T_C$ inducing high values of the Nernst constant seems accepted. Normally, vortex formation is expected at low temperatures. Ref. [52] explains how it is possible to offer an ideal explanation in the present approach.

5. 1. The magnetic 'neutron' resonance

We have shown [72] analytically that the magnetic 'neutron' resonance, generally known as the spin resonance in the literature, is a sharp resonant charge excitation, the plasmon of the dominant d-wave pairing band at its 2CKFP. It appears as a pole in the polarization of this band below the channel transition due to the reduced scattering in this regime. One can not truely separate spin and charge due to Pauli principle [44]. Due to the difficulty of detecting charge excitation [73], the excitation of the d-wave pairing band is usually detected by INS as a spin excitation.

The carrier at 2CKFP has spin ½, and is known to scatter other carriers via Coulomb interaction and spin-flip [74]. The assumption of 2CKFP makes it intrinsically possible for the d-wave pairing carrier to accommodate the spin flip, $\uparrow\downarrow\leftrightarrow\uparrow\uparrow$, which behaves as a doublet. We have verified [72] the data $(5\sim 5.5)k_BT_c \approx \Omega^o < \Omega^e < 2\Delta_0$ for the underdoped regime and $\Omega^o \approx \Omega^e \approx 2\Delta_0$ for the mildly overdoped regime. These results as well as others related to them were unexplained before. Ω^o and Ω^e are the odd and even symmetry excitations. The detailed and excellent consistency with two channel Kondo theory is outstanding.

5. 2. Penetration depth λ_C

For magnetic field applied along the c –direction of the crystal at 2CKFP λ_C has been calculated by us using the Matsubara technique,

$$\frac{1}{\lambda_C} \propto 1-(\frac{\pi}{12})(\frac{T}{\tilde{T}_K})^2[1-(\frac{7\pi^2}{30})(\frac{T}{\tilde{T}_K})^2-2\pi(\frac{\Delta}{\tilde{T}_K})^2 + (\frac{21\pi^3}{20})(\frac{T}{\tilde{T}_K})^2(\frac{\Delta}{\tilde{T}_K})^2] \quad (12)$$

Up to orders $(T/\tilde{T}_K)^2$ and $(\Delta/\tilde{T}_K)^2$. This gives $1/\lambda_C \propto -1/\tilde{T}_K{}^2 \propto -T_C{}^2$ within a constant for optimal doping when there is no large temperature variation. The second proportionality follows approximately from the phase diagram, figure 1. These results verifiy the data of ref. [75].

6. Axial conductivity and c-axis optical pseudogap

The c-axis tunnelling Green function of the d-wave superconductor at low frequencies is given in the normal state by $G_c(\vec{k},i\omega_n)^{-1}=\begin{pmatrix} G(\vec{k},i\omega_n)^{-1} & t_\perp \\ t_\perp & G(\vec{k},i\omega_n)^{-1}\end{pmatrix}$,

Where $t_\perp$ is the off-diagonal tunnelling matrix element. The procedure to obtain the above matrix equation is valid when the interlayer tunneling is much less than the coherence temperature, for the d-wave paring band. $G(\vec{k},i\omega_n)$ is the basal plane d-wave pairing band Green function. Note $\omega\sigma_c(\omega)=i\Phi_C(\omega)$ is an exact expression for any finite ω .

Using $\Phi_c(i\omega_p)=T\sum_n G(i\omega_n)G(i\omega_n-i\omega_p)$, in RPA within a constant multiplicative factor, and noting $\tilde{T}_{KC} >> t_\perp$ two possible approximations for $\sigma_C(\omega)$ obtained from $G_C(\vec{k},i\omega_n)$ are,

$$\sigma_C(\omega)=(\frac{-1}{2\pi\omega^2T})(\frac{\omega}{\tilde{T}_{KC}})^2\left[1+3\pi^2(\frac{T}{\tilde{T}_{KC}})^2\right],\ \omega<\tilde{T}_{KC}$$

$$\sigma_C(\omega)=(\frac{-1}{2\pi\omega^2T})\left[2\ln\frac{\omega}{\tilde{T}_{KC}}+\pi^2(\frac{T}{\tilde{T}_{KC}})^2(1+\frac{\tilde{T}_{KC}{}^2}{\omega^2})\right],\ \omega>\tilde{T}_{KC}\ . \quad (13)$$

(i) From the first line of eq. (13) for very small T and $\omega<\tilde{T}_{KC}$, $\sigma_C(\omega)\to-\infty$; secondly for $T\le\tilde{T}_{KC}$ and $\omega<\tilde{T}_{KC}$, $\sigma_C(\omega)\to$ a small negative value. That is, for temperature varying from zero to $\tilde{T}_{KC}$ $\sigma_C(\omega)$ changes by infinity. So , $\sigma_C(\omega)$ has a gap of width $\tilde{T}_{KC}$,the c-axis PG. This explains a never-understood mysterious piece of optical data [76]. (ii) Frequencies larger than $\tilde{T}_{KC}$ are ignored for low frequency work.

7. Superconducting order

7. 1. The stripe order

The physical need for the stripe transition that occurs in the PG regime is to allow two channel Kondo transition to take place via an effective nanoscale displacement of the oxygen atoms to the Cu site in the plane. This is required for the Kondo effect as the oxygen atoms harbour the doped holes. On the basis of this principle and proceeding by ignoring exhaustion effects explicitly [26, 77], it is possible to show that two holes in each cell at doping level p=1/8 lead to the structure of the stripe

that was first detected. It may be recalled that many-body correlation effect is already taken into account in Kondo effect.

This scenario, apparently naive but close to the facts, that clarifies the Kondo origin of the spin- and charge stripes can be presented as follows. Let us consider,for example, in the square lattice, say n×n, CuO_2 unit cells the top horizontal row of which is numbered 1,2,3,....*n*. Each unit cell has one Cu atom. Since for doping level p each cell has an average of p number of holes we need to collect all the holes from m unit cells to make up a complement of two holes per unit cell. That is, mp=2. So, m=2/p=16 is the required number of cells to provide two channel effect in one cell for p=1/8. But with due regard to the square symmetry of the crystal, we have to take the 16 cells as a 4×4 supercell. Thus, along both the rows and columns of unit cells m=4 is the correct number rather than 16. That is, m=1/2p. This shows that for p=1/8 in the antinodal direction there are three rows (or columns) of cells that have no holes at all followed by a fourth one where each cell has two holes. This enables two channel effect in such a cell and clarifies the relation between the doping level p=1/8 and the structure of the stripe. This should be taken as an indication of the validity of our Kondo picture of the origin of stripes.

7. 2. The checkerboard order

The checkerboard charge order of the crystal is a real space nanoscale nondispersive charge density modulation detected first near the vortex core of the HTC. It has been detected [78] in the superconductivity gap and in the PG as well [79]. Unlike the stripe order, this order depends on d-wave superconductivity of the crystal both in the dome and outside; the physics is very different from that of the stripe. Being nondispersive and incoherent, it is mainly in the antinodal area of the normal state. Stripe order, on the other hand, does not need superconductivity gap and may coexists in competition with superconductivity.

Our understanding based on data is that the checkerboard order is nothing other than the characteristic LDOS pattern which, in principle, each magnetic moment in the crystal can induce at 2CKFP under d-wave superconductivity. But a Zn impurity acts best in this respect. We have derived it [80] for Zn impurity which acts as a Kondo hole [81] at 2CKFP. We have shown that the decay length of the LDOS pattern scales as $\tilde{T}_K{}^2$. The decay length of the LDOS pattern which is defined as a quarter of the wave length of the checkerboard pattern has been calculated [80] to be about 30 Å. This agrees with data of Ref. [82], a work that presented,to our knowledge, the earliest example of the checkerboard pattern though the authors did not call it so.

Concluding this note , the multichannel Kondo effect enables the explanation of the whole corpus of experimental data on the HTC. Being also physically sound and with predictive power, it should be accepted as the true theory of the HTC. A brief analysis of experimental data on the more common HTC as well as some Hg-based compounds strongly suggests the fundamental involvement of this effect in their physics. One old idea that needs to be discarded is that of universality of the crystals; the idea is applicable to the CuO2 plane but not to the crystals as such. Even the very common data recorded for the HTC over several years ,if not ignored and overlooked , such as the residual entropy and resistivity of the crystals would have led to this conclusion earlier. Our conclusion has been again compellingly supported by recent Laser ARPES data on the doped cuprate. Preliminary work shows us that the same basic two channel Kondo physics is applicable to the Fe-based superconductors, the heavy fermion superconductors, the organic BEDT compounds, compounds of the family of 2H-$NbSe_2$ and other compounds listed by Uemura *et al.* [45].

Acknowledgement

Major part of the study reported here was done when the author was a visiting fellow at the Research Centre for Mathematical and Physical Sciences, Chittagong University, Bangladesh. This was made possible through the support, interest and enthusiasm of its then director, late Prof. J N Islam. Help and support of Prof. A. M. Choudhury, the present director, were invaluable to the author. Prof. H S Mani, director, The Harish Chandra Research Institute, Allahabad, India, was kind in inviting the author for a stay at his institute. The author has greatly benefited from a number of stays at the Abdus Salam ICTP, Trieste. He highly appreciates Prof. Ph Nozieres' of CNRS correspondence regarding the two channel Kondo effect. Prof. J R Waldram's kind comments on an earlier version of the manuscripts have been very helpful.

References

1. Y Ando *et al.*, *Phys. Rev. Lett*. **75** (1995) 4662.
2. S Ono *et al.*, *Phys. Rev. Lett.* **85** (2000) 638.
3. X G Luo *et al.*, *J. Superconducting Science & Technology* **18** (2005) 234.
4. F Rullier-Albenque *et al.*, *Europhys. Lett.* **81** (2008) 37008.
5. H Alloul *et al.*, *Phys. Rev. Lett.* **63** (1989) 1700.
6. M Takigawa *et al.*, *Phys. Rev.* B **43** (1991) 247.
7. M C Boyer *et al.*, *Nature Phys.* **3** (2007) 802.
8. Y Lubashevsky *et al.*, *Phys. Rev. Lett.* **106** (2011) 047002.
9. Y H Liu *et al.*, *Phys. Rev. Lett.* **101** (2008) 137003.
10. J P Carbotte *et al.*, *Nature* **401** (1999) 354.
11. D Manske *et al.*, *Phys. Rev. Lett.* **87** (2001) 177005.
12. A N Pasupathy *et al.*, *Science* **320** (2008) 196.
13. M Fabrizio *et al.*, *Phys. Rev. Lett.* **74** (1995) 4503.
14. M Fabrizio *et al.*, *J. Superconductivity* **9** (1996) 425.

15. P Nozieres and A Blandin, *J. Physique Fr.* **41** (1980) 193.
16. W Zhang *et al.*, *Phys. Rev.* B **85** (2012) 064514.
17. J M Bok *et al.*, *Phys. Rev.* B **81** (2010) 174516.
18. J H Yuan *et al.*, *Phys. Rev.* B **82** (2011) 104521.
19. H Y Choi *et al.*, *Front. Phys. (China)* **6**, 4 (2011) 440.
20. C M Varma, "*Notes on RVB-Vanila by Anderson et al., in Proc. NATO Advanced Research Workshop on New Challenges in Superconductivity: Experimental Advances and Emerging Theories*", Springer **183** (2005) 105.
21. Y He and C MVarma, *Phys. Rev. Lett.* **106** (2011) 14700.
22. D C Johnston, J Buschow K H (Ed.), "*Handbook of Magnetic Materials*", Elsevier, Amsterdam **10** (1997) 1.
23. C Pepin *et al.*, *Phys. Rev. Lett.* **98** (2007) 206401.
24. J W Loram *et al.*, *Phys. Rev. Lett.* **71** (1993) 1740.
25. C Niedermayer *et al.*, *Phys. Rev. Lett.* **80** (1998) 3843.
26. Ph Nozieres, *Eur. Phys. J.* B **6** (1998) 447.
27. S Sebastian *et al.*, *Phys. Rev.* B **81** (2011) 140505.
28. V J Emery and S Kivelson, *Phys. Rev.* B **46** (1992) 10812.
29. A M Sengupta and A Georges, *Phys. Rev.* B **49** (1994) 10020.
30. B Batlogg and V J Emery, *Nature* **382** (1996) 20.
31. H Fukuyama and H Kohno, "*Theory of high Tc cuprates: extended t-J model*", Proceedings of the 21st. Int'l Conference on Low Temperature Physics, Prague (1996).
32. E Pavarini, *Phys. Rev. Lett.* **87** (2001) 047003.
33. L Alff *et al.*, *Nature* **422** (2003) 698.
34. W S Lee *et al.*, *Nature* **450** (2007) 81.
35. J Haase, D Rybicki, and C P Slitcher *et al.*, *Arxiv*: 1110.6016.
36. H Y Hwang *et al., Phys. Rev. Lett*. **72** (1994) 2636.
37. M A Mojumder, *Physica* C **466** (2007) 148.
38. D van der Marel *et al.*, *Nature* **425** (2003) 271.
39. M Schlottman, *Phys. Rev. Lett.* **84** (2000) 1559.
40. M A Mojumder, *J. Superconductivity & Novel Magnetism* **23** (2010) 285.
41. C M Varma, L Zhu, *Phys. Rev. Lett.* **98** (2007) 177004.
42. K McElroy *et al.*, *Nature* **422** (2003) 592.
43. J Lee *et al.*, *Science* **325** (2009) 099.
44. C M Varma *et al.*, *Phys. Rep.* **361** (2002) 267.
45. Y J Uemura *et al.*, *Phys. Rev. Lett.* **66** (1991) 2665.
46. Y He and C M Varma, *Arxiv*: 1201.5828.
47. P Bourges and Y Sidis, *C R Phys.* (*Fr.*) **12** (2011) 461.
48. E van Heumen *et al.*, *J. Phys. Conf. Ser.* **150** (2009) 052278.
49. J Bäckström *et al., Phys. Rev.* B **70** (2004) 174502.
50. J Hwang *et al.*, *Phys. Rev. Lett.* **98** (2007) 207002.
51. E Elles *et al.*, *Phys. Rev.* B **79** (2009) 100505.
52. M A Mojumder, *Solid Stat. Commun*. **138** (2006) 371.
53. W Meevasana *et al.*, *Phys. Rev.* B **75** (2007) 174506.
54. W Meevasana *et al.*, *Phys. Rev.* B **77** (2008) 10450.
55. A Abrikosov *et al.*, "*Methods of quantum field theory in statistical physics*", Ed., R A Silverman, Dover (1963).
56. R Khasanov *et al.*, *J. Phys. Cond. Matter* **16** (2004) S4430.
57. R Khasanov *et al.*, *Phys. Rev.* B **74** (2006) 064504.
58. C Grimaldi *et al.*, *Europhys. Letters,* **42** (1998) 667.
59. T Timusk and B Statt, *Rep. Prog. Phys.* **62** (1999) 61.
60. M R Norman *et al.*, *Adv. Phys.* **54** (2005) 715.
61. M Hashimoto *et al.*, *Nature Physics* **6** (2009) 414.
62. O Fischer *et al.*, *Rev. Mod. Phys.* **79** (2007) 353.
63. A Bangura *et al.*, *Phys. Rev. Lett.* **100** (2008) 047001.
64. C Jaudet *et al.*, *Arxiv*: 1001.1508.
65. D LeBoeuf *et al.*, *Nature* **450** (2007) 533.
66. D Le Boeuf *et al.*, *Phys. Rev.* B **83** (2011) 054506.
67. M R Norman *et al.*, *Nature* **392** (1998) 157.
68. M A Mojumder, *J. Superconductivity & Novel Magnetism* **22** (2010) 417.
69. J M Harris *et al.*, *Phys. Rev. Lett.* **75** (1995) 1301.
70. M A Mojumder, *Physica* B **392** (2007) 361.
71. M A Mojumder, *Int. J. Mod. Phys.* **13** (1999) 3205.
72. M A Mojumder, *J. Superconductivity & Novel Magnetism* **22** (2010) 817.
73. H A Mook, F Dogan, *Nature* **401** (1999) 145.
74. H A Mook *et al.*, *Phys. Rev. Lett.* **70** (1993) 3490.
75. M R Trunin *et al.*, *Phys. Rev. Lett.* **92** (2004) 067006.
76. C Homes *et al.*, *Phys. Rev. Lett.* **71** (1993) 1645.
77. S Burdin *et al.*, *Phys. Rev. Lett.* **85** (2000) 104.
78. J E Hoffman *et al.*, *Science* **295** (2002) 466.
79. M Vershinin *et al.*, *Science* **303** (2004) 1995.
80. M A Mojumder, *Europhys. Lett.* **62** (2003) 575.
81. R Sollie, P Schlottman, *J. App. Phys.* **70** (1991) 5803.
82. S H Pan *et al.*, *Nature* **403** (2000) 746.